arXiv:1104.2924v2 [cond-mat.quant-gas] 5 Jul 2011

Anomalous Dimers in Quantum Mixtures near Broad Resonances: Pauli Blocking, Fermi Surface Dynamics and Implications

Jun-Liang Song
Institute for Quantum Optics and Quantum Information of the Austria Academy of Sciences, A-6020 Innsbruck, Austria

Fei Zhou
Department of Physics and Astronomy, University of British Columbia, Vancouver, B.C., Canada V6T1Z1

(Dated: June 13, 2011)

We study the energetics and dispersion of anomalous dimers that are induced by the Pauli blocking effect in a quantum Fermi gas of majority atoms near interspecies resonances. Unlike in vacuum, we find that both the sign and magnitude of the dimer masses are tunable via Feshbach resonances. We also investigate the effects of particle-hole fluctuations on the dispersion of dimers and demonstrate that the particle-hole fluctuations near a Fermi surface (with Fermi momentum $\hbar k_F$) generally reduce the effective two-body interactions and the binding energy of dimers. Furthermore, in the limit of light minority atoms the particle-hole fluctuations disfavor the formation of dimers with a total momentum $\hbar k_F$, because near $\hbar k_F$ the modes where the dominating particle-hole fluctuations appear are the softest. Our calculation suggests that near broad interspecies resonances when the minority-majority mass ratio m_B/m_F is smaller than a critical value (estimated to be 0.136), dimers in a finite-momentum channel are energetically favored over dimers in the zero-momentum channel. We apply our theory to quantum gases of ^{6}Li^{40}K, ^{6}Li^{87}Rb, ^{40}K^{87}Rb and ^{6}Li^{23}Na near broad interspecies resonances, and discuss the limitations of our calculations and implications.

I. INTRODUCTION

Pairing of fermions or electrons in quantum condensed matter systems for long has been one of the most remarkable phenomena discovered in many-body physics [1–3]. It is also the fundamental issue in the so-called color-superconductivity phenomenon in the core of a neutron star [4]. Recent developments in the field of ultracold atoms, especially the observation of atomic Feshbach resonances, have further led to tremendous new opportunities of studying novel pairing correlations in quantum gases [5–8]. Because of tunability of interactions and availability of a rich variety of alkali isotopes, cold gases have been turned into a marvelous, promising platform to study diversified pairing phenomena with unique correlations. Pairing properties near Feshbach resonances are mainly determined by, apart from scattering lengths, asymmetries in chemical potentials of the different atoms involved. Such asymmetries and consequently a very rich class of pairing phenomena are known either due to the imbalance in populations [6–14] or tunable mass ratios [15–18], or both. Moreover, differences in the quantum statistics of underlying atoms also contribute to the asymmetries in chemical potentials as in Fermi-Bose mixtures [19–26]. Previous theoretical studies on Fermi- Bose mixtures have been focused on the formation of molecular Fermi surfaces near narrow resonances [27] or far away from resonances [28], pair correlations [29], and quantum and thermal depletion of condensates [30].

A very closely related fascinating issue that has been challenging to the cold atom community is whether near-resonance two-body scattering in a channel with nonzero total momentum dictates the instability in interacting quantum mixtures. A major challenge in the studies of pairing phenomena in various quantum mixtures near resonances, unlike in the BCS-BEC crossover regime of a Fermi gas, is that there are more competing pairing schemes and possibilities of having higher order correlations; energetically it is quite difficult to differentiate competing scenarios near resonances. One natural approach is of course to perform a full-scale numerical simulation to resolve the issue. An alternative is perhaps to study few-body physics in the presence of a finite-density quantum gas and to gain insight on many-body correlations by exploring implications of few-body physics. A few interesting attempts have already been made along this direction. For instance, the properties of a single minority atom submerged in a quantum Fermi gas have been thoroughly investigated as a diagnosis of many-body correlations near interspecies Feshbach resonances [31–38]. For Fermi-Bose mixtures, anomalous dimers with tunable masses were emphasized and the leading effect of particle-hole fluctuations had been studied diagrammatically [39]. At the same time, for Fermi-Fermi mixtures various instability lines have been determined numerically by studying the dimer and trimer formation in a truncated Hilbert space and the role of anomalous dimers as well as a universal trimer was explored [18]. And very recently, Efimov states in a Fermi gas were studied in a few limiting cases and the spectrum flow has been obtained in the static-Fermi-sea approximation [40]. Logically speaking, these studies should form potential building blocks for constructing many-body states; they can also serve as a starting point for more systematic studies on the interplay between few- and many-body physics in cold gases near resonances.

In this paper, we take a further step along this direction hoping that our efforts to understand dressed bound states can shed more light on many-body pairing phenomena in mixtures. Particularly, we consider the limit of *a single atom or a minority atom in resonance with majority Fermi atoms which form a Fermi sea.* This minority atom can be either a fermion or boson although most of our discussions are in the context of a Bose atom resonating with a Fermi sea. We obtain the dispersion of dimers and investigate the Pauli blocking effect, the effect of fluctuating particle-hole pairs near the Fermi surface on the dimer energetics. These results should be applicable to quantum mixtures with extremely imbalanced population. We further examine the dimer dispersion near broad interspecies resonances for ^{6}Li-^{87}Rb [41, 42], ^{6}Li-^{23}Na [19, 43], ^{40}K-^{87}Rb [20–26] and ^{6}Li-^{40}K [44–46] that have been available in laboratories.

Our analysis on the dispersion of dimers further suggests that when the minority atom is very light, minority-majority atoms near broad resonances would prefer to form dimers in finite-momentum channels that are energetically favorable. Although quantum mixtures of ^{6}Li-^{40}K, ^{6}Li-^{87}Rb, ^{40}K-^{87}Rb and ^{6}Li-^{23}Na so far studied in laboratories are not in this particular limit, we anticipate such a limit can be explored in future generations of quantum mixtures. More importantly, when combining the optical lattices and Feshbach resonances [24, 47], one can achieve resonances with continuously tunable widths and locations [48]. By properly choosing laser intensities, or by using isotope selective optical lattices [47], the ratio of band masses of Fermi-Bose atoms can be further continuously tuned over a very wide range. This leads to potential opportunities of studying the limit of light Bose atom.

The rest of the paper is organized as follows. In Sec. II, we introduce the model Hamiltonian for broad resonances and study the formation of dimers in a static Fermi sea. We analyze the effects of Pauli blocking on the dispersion of dimers, and illustrate that a kinematic effect in the limit of very light minority atoms favors finite-momentum dimers near broad resonances. We then present the results for quantum mixtures so far studied in laboratories. In Sec. III, we go beyond the static-Fermi-sea approximation to take into account various corrections due to particle-hole fluctuations near the Fermi surface of majority fermions. Our calculations indicate that the main effect of fluctuating pairs is to reduce the binding energy of dimers and also to disfavor the formation of dimers with total momenta close to $\hbar k_F$. In Sec. IV, we discuss the limitations of our results, explore the implications on near-resonance quantum mixtures with a finite density of minority atoms and comment on various results [14, 15, 18, 39, 40] obtained in previous studies. We summarize the results and discussions in Sec. V.

II. ANOMALOUS DIMERS: PAULI BLOCKING EFFECT

We start with a single-channel Hamiltonian with a short-range interaction U_{bf} that was introduced previously for a study of Fermi-Bose mixtures near broad resonances [39],

$$\begin{aligned} H &= \sum_{\mathbf{k}} \epsilon^F_{\mathbf{k}} f^\dagger_{\mathbf{k}} f_{\mathbf{k}} + \sum_{\mathbf{k}} \epsilon^B_{\mathbf{k}} b^\dagger_{\mathbf{k}} b_{\mathbf{k}} \\ &+ \frac{U_{bf}}{\Omega} \sum_{\mathbf{k},\mathbf{k}',\mathbf{Q}} f^\dagger_{\frac{m_R}{m_B}\mathbf{Q}+\mathbf{k}} b^\dagger_{\frac{m_R}{m_F}\mathbf{Q}-\mathbf{k}} f_{\frac{m_R}{m_B}\mathbf{Q}+\mathbf{k}'} b_{\frac{m_R}{m_F}\mathbf{Q}-\mathbf{k}'} \end{aligned} \quad (1)$$

Here $f^\dagger_{\mathbf{k}}$,$b^\dagger_{\mathbf{k}}$($f_{\mathbf{k}}$,$b_{\mathbf{k}}$) are creation (annihilation) operators for Fermi and Bose atoms respectively, and $\epsilon^{F(B)}_{\mathbf{k}} = \frac{\hbar^2|\mathbf{k}|^2}{2m_{F(B)}}$ are kinetic energies for fermions (bosons) and Ω is the volume. U_{bf} is the strength of short-range interaction between fermions and bosons, and is equal to scattering lengths $2\pi\hbar^2 a/m_R$ after regularization [39] (see also Appendix A). And $m_R = m_B m_F/(m_B + m_F)$ is the reduced mass, $\epsilon^R_{\mathbf{k}} = \hbar^2|\mathbf{k}|^2/2m_R$. This single-channel model effectively describes near-resonance physics provided the resonance is broad enough; i.e., the effective range is much smaller than the Fermi wavelength [49].

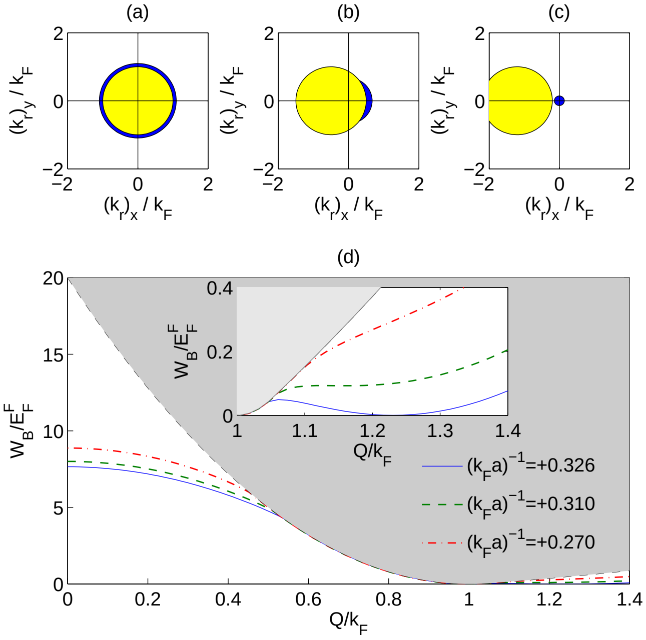

FIG. 1: (Color online) (a)–(c) Schematics of the Pauli blocking effect on dimers with total momentum $|\hbar\mathbf{Q}| = 0$, $0.2(m_B/m_R)\hbar k_F$, $(m_B/m_R)\hbar k_F$, respectively. Yellow (light gray) areas in the relative momentum k_r space are for the blocked or occupied states and blue (dark gray) areas stand for states available for pairing near the threshold of the two-body continuum. (d) Energy dispersion of excited dimers for the mass ratio $m_B/m_F = 0.05$; shown in the inset is the part of dispersion for $|\mathbf{Q}| > k_F$. Shaded areas are for the two-atom excitation continuum. At $1/k_F a = 0.326$, the minimum of dispersion reaches zero energy at a finite momentum $\hbar Q_{min} = 1.23\hbar k_F$. Beyond this point, a dimer should appear in the ground state when a minority atom nearly resonates with a Fermi sea.

To get insight into pairing with a nonzero total momentum $\hbar\mathbf{Q}$, we examine the dispersion for a two-body

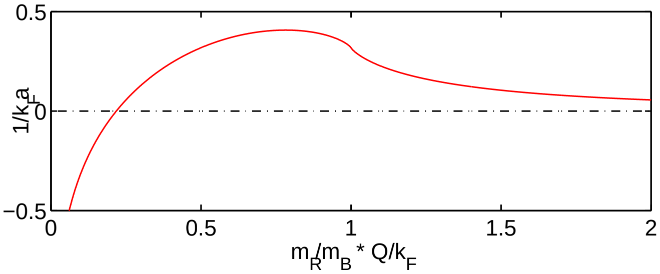

FIG. 2: (Color online) For a dimer with total momentum $\hbar Q$ to appear in the two-body excitation spectrum, $1/(k_F a)$ has to exceed a minimum value indicated by the curve. Dashed line is for free space without a Fermi sea.

bound state of Fermi-Bose atoms with an arbitrary total momentum $\hbar\mathbf{Q}$ or a center-of-motion kinetic energy $\epsilon^C_{\mathbf{Q}} = \hbar^2\mathbf{Q}^2/2m_T$ and $m_T = m_F + m_B$. The dispersion can be obtained by solving the two-body problem on top of a "frozen" Fermi sea of majority atoms. The resultant self-consistent equation is

$$\frac{-m_R}{2\pi\hbar^2 a} = \frac{1}{\Omega}\sum_{\mathbf{k}}\left[\frac{\Theta(|\frac{m_R}{m_B}\mathbf{Q}+\mathbf{k}|-k_F)}{\epsilon^R_{\mathbf{k}}+\epsilon^C_{\mathbf{Q}}-\epsilon^F_F-W_B(\mathbf{Q})}-\frac{1}{\epsilon^R_{\mathbf{k}}}\right], \quad (2)$$

Here $W_B(\mathbf{Q})$ is the energy of dimers with momentum $\hbar\mathbf{Q}$, and is measured from the Fermi energy $\epsilon^F_F = \hbar^2 k_F^2/2m_F$ of majority atoms. The unit step function $\Theta(\cdots)$ in the sum excludes occupied states below the Fermi surface.

This equation can also be obtained by studying the scattering matrix in the presence of a Fermi sea; the pole of the T matrix on the real axis, if it exists, corresponds to a bound state with an infinite lifetime (see Appendix A). We find that Eq.2 is very similar to the well-known Cooper's solution to two attractive electrons on the top of a Fermi sea[50]. Note that the T matrix approach usually yields an additional contribution to the Cooper's original solution due to the inclusion of hole like configurations in the eigenvalue equation. However, since here we are dealing with a situation where only a single minority atom resonates with majority ones and there is no minority Fermi sea, in our case the hole like configurations do not contribute to the binding energy.

The presence of a Fermi surface leads to an anomalous dimer excitation spectrum when the scattering length is small and negative. Two interesting aspects of the dispersion are worth emphasizing. First, dimers with zero momentum appear in the form of excitations for arbitrary negative scattering lengths even when they are small in magnitude. On the contrary, dimers with a finite momentum can exist only when the scattering lengths exceed a critical value. In fact, due to the Pauli blocking effect, the threshold of two-body continuum for a total momentum $\hbar\mathbf{Q}$ is

$$\begin{aligned} E_{th}(\mathbf{Q}) &= \frac{\hbar^2|\mathbf{Q}|^2}{2m_T}+\frac{\hbar^2 q^2_{min}}{2m_R}-\epsilon^F_F \\ q_{min} &= \max(k_F-\frac{m_R}{m_B}|\mathbf{Q}|,0). \end{aligned} \quad (3)$$

This is different from the case in vacuum where $E^{vac}_{th}(Q) = \frac{\hbar^2 Q^2}{2m_T}$. As a result for $Q = 0$, one finds that the available density of states $D_{2b}(E)$ for two-body scattering does not vanish when E approaches E_{th}. When $0 < |\mathbf{Q}| < \frac{m_B}{m_R}k_F$, one finds that $D_{2b}(E)$ always vanishes linearly as a function of energy $E - E_{th}$, i.e.

$$D_{2b}(E) = \frac{m_B^2 k_F}{4\pi^2}\frac{E-E_{th}}{Q\left(\frac{m_B k_F}{m_R}-Q\right)}. \quad (4)$$

The qualitative difference between $D_{2b}(E)$ for the zero-momentum channel and for the finite-$\mathbf{Q}$ channels is schematically illustrated in Figs. 1(a)–(c). Note that near the threshold, the two-atom scattering states with zero total momentum $Q = 0$ are represented by the whole shell around the Fermi surface while the scattering states with finite total momenta only correspond to a small strip around the Fermi surface. The relatively low density of states near E_{th} for finite-Q scattering puts a severe constraint on the formation of dimers with a finite momentum. And for a given negative scattering length, we find that dimers only appear in the spectrum up to a maximum total momentum. This is reflected in Fig.1(d) in which the dimer dispersion ends up at a finite momentum and merges into the two-atom scattering continuum. Alternatively, one can conclude that to form a finite-momentum molecule, the value of $(k_F a)^{-1}$ has to exceed a minimum value as shown in Fig.2.

Second, the dispersion minimum might locate at a finite center-of-mass momentum $\hbar\mathbf{Q}$. And this is the case either when atoms are away from resonances with small negative scattering lengths or when Bose atoms are very light. In the former case, it is due to the decreasing threshold E_{th} as the momentum Q increases from zero and therefore the energy of bound states below the threshold (see Fig. 1). In the latter situation, to form a molecule with zero total momentum $\hbar\mathbf{Q} = 0$ Bose atoms need to be promoted at least to right above the Fermi surface resulting in a high energy penalty ϵ^B_F, while to form a molecule with total momentum near $\hbar k_F$ Bose atoms need not to be elevated. So energetically it could be more favorable to have molecules of Fermi-Bose atoms with a nonzero total momentum $\hbar\mathbf{Q}$ in this limit.

We have examined m_{eff}, the effective mass of extended dimers near $Q = 0$, as a function of scattering length a and the mass ratio m_B/m_F. At any small negative scattering length $[-(k_F a)^{-1} \gg 1]$ or far away from resonances,

$$\frac{1}{m_{eff}} = -\frac{m_R}{6m_B^2}\exp\left(-\frac{\pi}{k_F a}\right) \quad (5)$$

and it is indeed always negative. At scattering lengths $a^{(I)}$ where creation of a dimer with zero momentum costs no energy or $W_B(Q = 0) = 0$, we find that

$$\frac{1}{m_{eff}} = \frac{1}{m_T}\left[1-\frac{4m_F}{3m_B}g\left(\sqrt{\frac{m_R}{m_F}}\right)\right]; \quad (6)$$

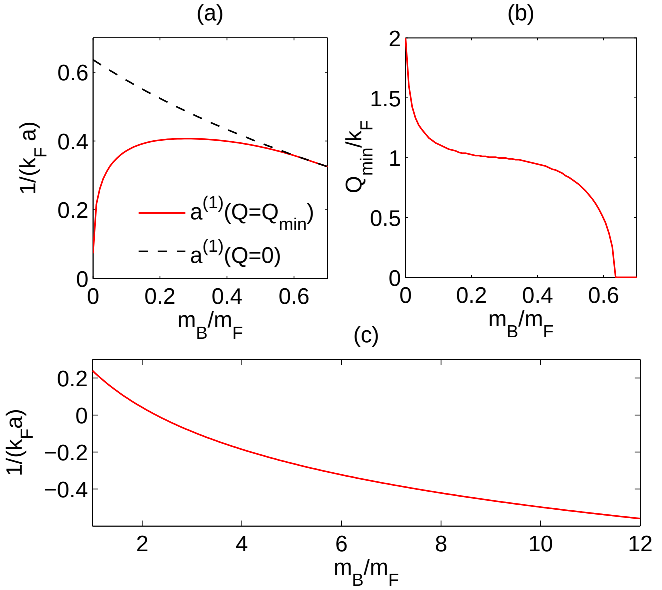

FIG. 3: (Color online) (a) Critical values of a at which the dimer excitation energy $W_B(\mathbf{Q})$ becomes zero at $Q = Q_{min}$, the minimum of the excitation spectrum; a dimer starts emerging in the ground state for a minority atom resonating with a Fermi sea beyond this line. The dashed line is obtained by setting $W_B(0) = 0$ or for the scattering lengths at which the zero-momentum dimer energy vanishes. (c) is for larger mass ratios. (b) Q_{min}, the momentum at which the dimer dispersion touches zero for the first time when approaching the resonance from the side of negative scattering lengths, as a function of mass ratio m_B/m_F. These plots are obtained assuming the Fermi surface is static and there are no particle-hole fluctuations.

and the dimensionless function

$$\frac{1}{g(x)} = \left(1 - x^2\right)\left[2 + \frac{1 - x^2}{x} \ln \frac{1 + x}{1 - x}\right]. \tag{7}$$

Note that m_{eff} in Eq.6 is an indicator of relevance or irrelevance of zero-momentum dimers when dimers start appearing in the ground state near resonance. And as far as $m_B/m_F > 0.7$ and the energy penalty ϵ_F^B is not too heavy, m_{eff} is positive, although it can be much bigger than the bare mass $m_T (= m_F + m_B)$ as a result of dressing in the Fermi sea. In this limit, the dimer spectrum indeed crosses zero first at $Q = 0$ and a zero momentum dimer is expected to appear in the ground state. However, when $m_B < 0.7 m_F$, the effective mass becomes negative, implying the relevance of dimers with finite momenta in the reconstructed ground state. Indeed we find that for small mass ratios, the minimum of the dispersion spectrum crosses zero first at a finite momentum $\hbar Q_{min}$ when approaching resonances from the side of negative scattering lengths. Going further beyond this point, one would expect that dimers with finite momenta $\hbar Q_{min}$ thus appear in the ground state for minority atoms resonating with a Fermi sea. Details are shown in Fig. 3. In Figs. 4–5, we also present the results for dimers near a few broad interspecies resonances that have been studied in recent experiments.

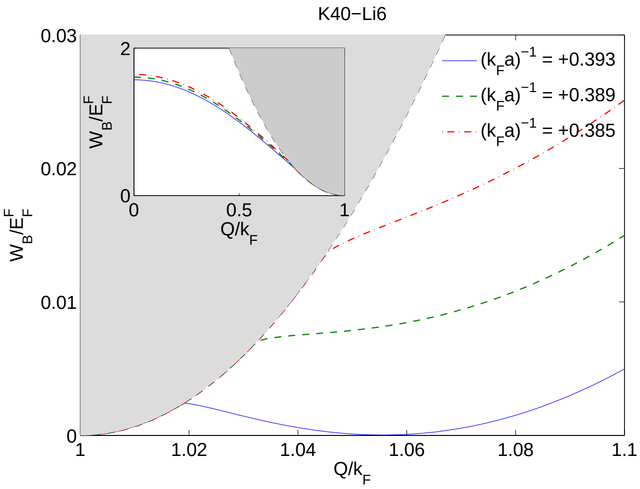

FIG. 4: (Color online) Energy dispersion of dimers near an interspecies resonance of ^{6}Li-^{40}K atoms. $m_B/m_F = 0.15$ for a ^{6}Li atom nearly resonating with a Fermi sea of heavy ^{40}K atoms. Shaded areas are again for two-atom excitation continuum. At $1/k_F a = 0.393$, the minimum of dispersion reaches zero energy at a finite wave vector $Q_{min} = 1.05 k_F$.

III. EFFECT OF FLUCTUATING PARTICLE-HOLE PAIRS NEAR THE FERMI SURFACE

Besides the Pauli blocking effects, the energetics of bound states can be further modified by the dynamics of Fermi seas, or virtual particle-hole pairs near the Fermi surfaces, so the dimers are further dressed in fluctuating particle-hole pairs. One of the main effects of these fluctuating pairs is to renormalize the two-body interactions near the Fermi surface and therefore to modify the binding energetics of dimers as well as the dispersion. The fluctuating particle-hole pairs also lead to a decay of the dimer into either another lower energy dimer or two unbound atoms in the continuum and we will not discuss the decay in this paper [51].

The main effect on two-body scattering and therefore the dimer binding energy is illustrated in Fig.6, both schematically and diagrammatically. Consider a general situation where the density for minority atoms or Bose atoms is finite but much smaller than the density of majority Fermi atoms [52]. Three classes of particle-hole pair fluctuations contribute:

(A) A majority Fermi atom is first excited from below the Fermi surface to above by the incoming colliding minority Bose atom; the Fermi hole is later filled by the incoming Fermi atom that simultaneously scatters the minority Bose atom to its final state.

(B) A minority Bose atom is excited from the condensate by the incoming colliding majority Fermi atom; the

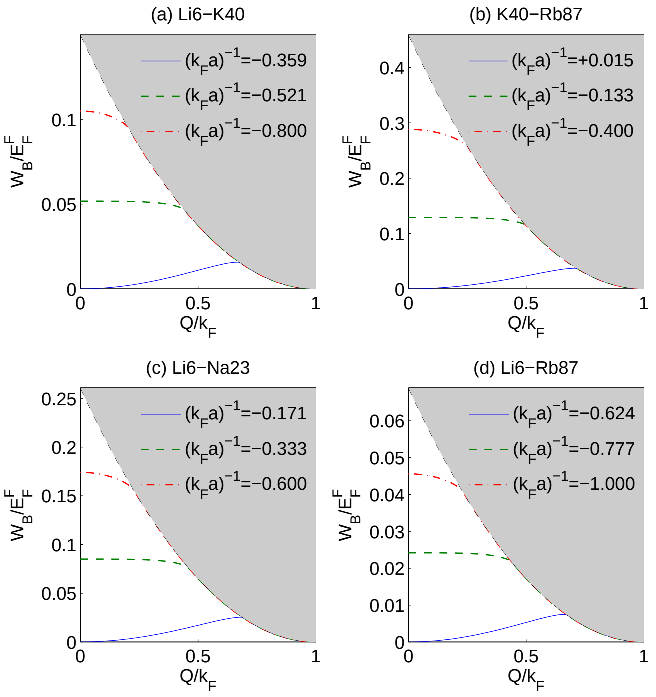

FIG. 5: (Color online) Energy dispersion of dimers for different mass ratios. (a) $m_B/m_F = 6.67$ for a single ^{40}K atom resonating with a Fermi sea of light ^{6}Li atoms; (b) $m_B/m_F = 2.175$ or for an interspecies resonance between ^{40}K and ^{87}Rb atoms; (c) $m_B/m_F = 23/6$ or ^{6}Li-^{23}Na resonance; (d) $m_B/m_F = 14.83$ or ^{6}Li-^{87}Rb resonance. In (b)–(d), minority atoms are Rb, Na, and Rb atoms, respectively. Shaded areas are again for two-atom excitation continuum. In (a)–(d), the minimum of dispersion first reaches zero energy at zero momentum.

Bose hole is later filled by the incoming Bose atom that simultaneously scatters the Fermi atom to its final state.

(C) A majority Fermi and a condensed Bose atom are excited with holes left behind filled in later by the incoming majority Fermi and minority Bose atoms.

A- and C-class processes involve exchange of virtual Fermi particle-hole pairs; i.e., a second majority Fermi atom has to be ejected out of the Fermi sea; they both have an additional negative sign with respect to the processes in class B (see Fig. 6) or the direct processes without virtual particle-hole pairs. One can also carry out a parallel analysis on a Fermi-Fermi mixture by replacing a condensate with a Fermi sea of minority atoms. In that case, the processes in the A-class or B-class will have a different sign with respect to the processes in the C-class as well as the direct scattering. And in the limit of a single minority atom that we are going to focus on or when the minority atom density vanishes, only the processes in the A-class contribute.

To understand this particular energetic effect of fluctuating particle-hole pairs, we study the T matrix including vertex corrections due to these fluctuating pairs. The technical details of this part are summarized in Appendix B. Scattering with the Fermi sea effectively takes momenta away from the incoming minority atom of the dimer to create virtual particle-hole pairs. This virtual process crucially depends on the initial and final relative momentum between the two atoms in the dimer. This can been illustrated via a momentum flow chart in Eq. (8) for two incoming atoms with the total momentum $\hbar\mathbf{Q}$ and relative momentum $\hbar\mathbf{k}$ scattered into two outgoing atoms with the same total momentum but different relative momentum $\hbar\mathbf{k}'$ through colliding with the Fermi surface.

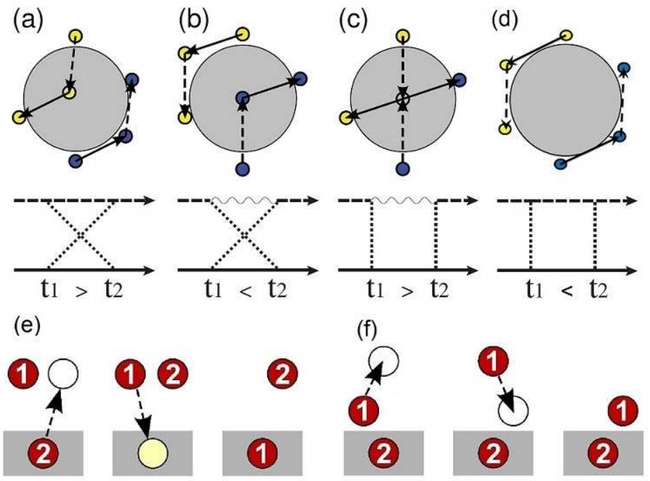

FIG. 6: (Color online) An illustration of induced scattering by virtual particle-hole pairs near a Fermi surface (a), a condensate (b), or both (c). (d) is for direct scattering without virtual particle-hole pairs. In (a)–(d), a minority atom [blue(dark gray) dots] and majority atoms [yellow(light gray) ones] have an interspecies resonance with zero total momentum; the light blue (light gray) area represents states occupied by fermions. Also shown is a diagrammatic representation of induced scattering with the time order illustrated explicitly. Solid line is for Fermi atoms, dashed line is for minority Bose atoms with nonzero momentum, and wavy lines are for Bose atoms in a condensate. In (e) and (f), we also illustrate two distinct virtual processes in (a)–(d): (a) and (c) involve, in addition to the incoming Fermi atom, a hole below the Fermi surface [as shown in (e)] while (b) or (d) does not [see (f)]. Because of the Fermi exchange statistics, the amplitude of the (e) process has an additional negative sign with respect to that of the direct process (d) as well as that of the (f) process. In the single-minority-atom limit, only A-class and the direct processes contribute; the dashed line can also represent a minority Fermi atom in this limit.

$$
\begin{aligned}
& f^\dagger_{\frac{m_R}{m_B}\mathbf{Q}-\mathbf{k}} b^\dagger_{\frac{m_R}{m_F}\mathbf{Q}+\mathbf{k}} |F.S.\rangle \rightarrow \\
& f^\dagger_{\frac{m_R}{m_B}\mathbf{Q}-\mathbf{k}} b^\dagger_{\frac{m_R}{m_F}\mathbf{Q}+\mathbf{k}-\mathbf{q}} f^\dagger_{\frac{m_R}{m_B}\mathbf{Q}-\mathbf{k}'} f_{\frac{m_R}{m_B}\mathbf{Q}-\mathbf{k}'-\mathbf{q}} |F.S.\rangle \rightarrow \\
& f^\dagger_{\frac{m_R}{m_B}\mathbf{Q}-\mathbf{k}'} b^\dagger_{\frac{m_R}{m_F}\mathbf{Q}+\mathbf{k}'} |F.S.\rangle \qquad (8)
\end{aligned}
$$

where $|F.S. >$ is introduced to represent the Fermi sea of majority fermions; the virtual state energy explicitly depends on $\mathbf{Q}, \mathbf{k}, \mathbf{k}'$. So with the particle-hole fluctuations, the T matrix not only depends on the total momentum $\hbar\mathbf{Q}$ but also the relative momentum $\hbar\mathbf{k}$ and $\hbar\mathbf{k}'$. Effectively, the fluctuating pairs mediate an interaction with a finite range.

One of the ways to estimate these effects is to introduce an effective scattering length (see Appendix B for details). The effective scattering length $\tilde{a}$ can be expressed as

$$\tilde{a}^{-1} \ = \ a^{-1} - k_F R + O(k_F^2 a)..., \tag{9}$$

Here $\tilde{a}$ differs from the free space scattering length a due to the particle-hole pair fluctuations. And $k_F R$ represents the lowest order vertex correction induced by fluctuating particle-hole pairs near a Fermi surface (or in condensates if a finite density of minority Bose atoms are present, or both) as shown in Fig. 6 (see also Appendix B). This correction is analogous to the vertex corrections discussed for zero-momentum pairing in fermion superfluids by Gor'kov and Melik-Barkudarov [53]. We shall denote this correction as the GMB vertex corrections (see also [52]) in the following discussion. Here we have carried out a detailed diagrammatic analysis on the GMB correction in finite-Q channels. We obtain the momentum dependence of induced scatterings and summarize the main results below. As a remark, we find that in the limit of heavy minority atoms (large mass ratio m_B/m_F), the R function for two-atom scattering with zero total momentum is

$$R \rightarrow \frac{1}{\pi} \log \frac{m_B}{m_F}. \tag{10}$$

We use natural logarithmic functions with base e here and throughout the paper. This logarithmic divergence in the large-mass-ratio limit can be attributed to the very heavy dressing of a zero-momentum dimer in virtual particle-hole pairs near the Fermi surface. One can also demonstrate that this has the same origin as the Anderson's infrared catastrophe in a quantum impurity problem [54].

We have numerically found that for scatterings near the threshold of two-particle continuum, the exchange processes in the A-class described above always induce an effective *repulsive* interaction. So the fluctuating particle-hole pairs in this case effectively *screen* or *reduce* the interspecies attractive interactions in all channels of momenta $\hbar\mathbf{Q}$ (see Fig.7). Furthermore, the *magnitude* of the corrections to the effective two-atom scattering strongly depends on the total momentum $\hbar\mathbf{Q}$ of the scattering atoms. This can be demonstrated by explicitly examining two cases: $\hbar Q = 0$ and $\hbar Q = \hbar k_F$ in the limit of *light* minority atoms, i.e., when the energy of virtual states is dominated by the minority atom. For a pair of minority and majority atoms in the $\hbar Q = 0$ channel, or with momentum $(\hbar\mathbf{k}, -\hbar\mathbf{k})$, it requires that the minority atom momentum be close to $\hbar k_F$ because of the Pauli blocking effect. Consider such an incoming minority atom with momentum $\hbar\mathbf{k}$ colliding with the Fermi surface popping up a pair of particle-hole excitation. The intermediate virtual state with total energy ϵ_v, and total momentum $\hbar\mathbf{k}$ consists of an outgoing minority atom and a particle-hole pair of majority atoms. This energy ϵ_v can be either larger or smaller than the energy of the incoming minority atom $\epsilon^B_{\mathbf{k}}$. The contribution to the effective interactions from a virtual state of energy ϵ_v is inversely proportional to $\epsilon^B_{\mathbf{k}} - \epsilon_v$ and so the contributions from different virtual states would have different signs depending on whether $\epsilon^B_{\mathbf{k}}$ is larger or smaller than ϵ_v, thus leading to a destructive interference between different configurations. Now let us turn to the scattering channel with the total momentum near $\hbar|\mathbf{Q}| = \hbar k_F$, i.e. a minority atom with $\hbar\mathbf{k} = 0$ interacting with a majority atom near the Fermi surface with Fermi momentum $\hbar k_F$. For a minority atom with $\epsilon^B_{\mathbf{k}} = 0$, *all* intermediate virtual states would have energies larger than the initial one and all should contribute to the effective interaction with the same sign, leading to a constructive interference. This results in a maximum value of the correction to two-body interactions; i.e., the correction reaches a peak value when $\hbar\mathbf{k}$ is near zero or $\hbar|\mathbf{Q}|$ is near $\hbar k_F$.

A more elaborated examination along this line can be carried out in Appendix B. There we show that for all virtual states involving a hole like excitation of momentum $\hbar\mathbf{l}$, the most dominating contribution to the overall vertex correction is always from the state with $\hbar\mathbf{l} \simeq \hbar k_F \mathbf{Q}/|\mathbf{Q}|$ so that the energy difference between the virtual state and the initial state is minimum. We can further introduce an effective *group* velocity for virtual states involving a hole like excitation with momentum as $\hbar\mathbf{l}$, $\partial\epsilon_v(\mathbf{l})/\partial\mathbf{l}$. For the scattering near the threshold of the two-body continuum, this velocity turns out to be proportional to $m_R/m_B Q - k_F$. In the limit of light minority atoms, i.e., the reduced mass m_R approaches m_B, the dominating virtual states appear softest near $\hbar Q = \hbar k_F$, consistent with the above qualitative argument based on interference effects. In general, formation of bound states near $\hbar Q = (m_B/m_R)\hbar k_F$ is disfavored by the fluctuating particle-hole pairs. For this reason, the vertex correction to two-body interactions due to the creation of particle-hole pairs is relatively small near small and large total momentum, and peaks near $\hbar Q = \hbar k_F$ in the limit of light minority atoms. This is confirmed in our numerical evaluations of R. So fluctuating particle-hole pairs favor the formation of dressed bound states with $\hbar Q$ away from $\hbar k_F$, over the dimers with $\hbar Q \simeq \hbar k_F$. Note that although we arrive at this conclusion by considering only the lowest order corrections, we conjecture that this is generically true as far as the effective group velocity for the hole like excitations has a minimum near $\hbar Q = \hbar k_F$. The position of the peak in Fig.7 in our opinion correlates with the threshold minimum where the screening effect is usually the strongest.

The problem of two-atom scattering near $\hbar Q = \hbar k_F$ is closely related to the spin polaron in cold gases that has been discussed quite extensively in the recent literature[31–38]. In our calculation, we also see a transition from a polaron to dimer when approaching the resonance from the negative-scattering-length side. We refer the readers to those publications for more elaborated discussions on the spin polaron. However, we should also emphasize that although the physics of the spin polaron itself is an interesting subject, to understand the nature of the ground state of a single minority atom; or the general pairing correlations in quantum mixtures near resonances, it is necessary to study the whole dimer spectrum. This is because as we have seen before, the minimum of the dispersion can occur at any momentum depending on the mass ratio $\frac{m_B}{m_F}$. The minimum location $\hbar Q_{min}$ generally differs from $\hbar Q = \hbar k_F$ or $\hbar Q = 0$. Only for a certain range of mass ratios, scatterings near $\hbar Q = 0$ or $\hbar Q = k_F$ set the overall instability of a unpaired minority atom.

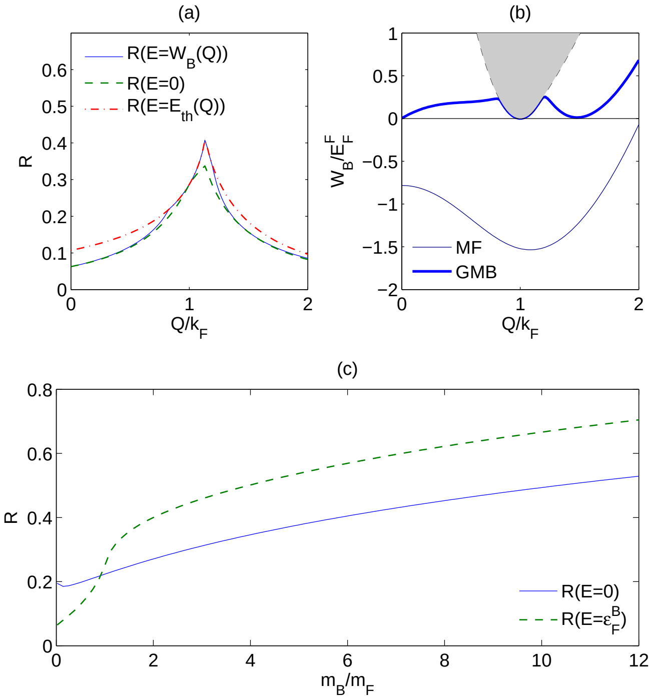

FIG. 7: (Color online) (a) R, the vertex correction as a function of total momentum $\hbar Q$ for mass ratio $m_B/m_F = 0.135$. Here the parameter R is defined as $1/k\tilde{a} = 1/k_F a - R$. Different plots are obtained with different choices of energy E; the solid line is obtained using a self-consistent method where $E = W_B(Q)$. (See more discussions in Appendix B.) (b) Dispersion of dimers with GMB and without MF particle-hole fluctuations or formally Gorkov-Melik-Barkudarov (GMB) vertex corrections for $m_B/m_F = 0.135$ and $(k_F a)^{-1} = 0.62$. (c) R for the $Q = 0$ scattering channel as a function of mass ratio m_B/m_F.

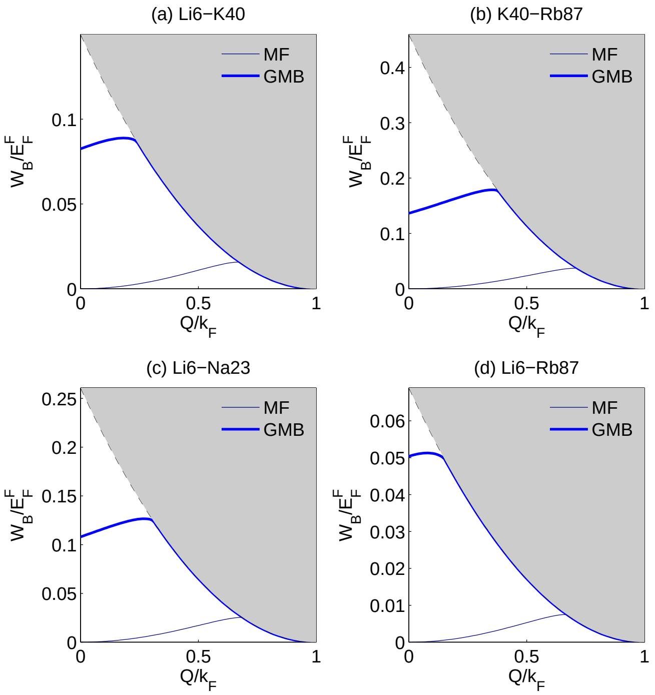

FIG. 8: (Color online) The vertex corrections to the dimer spectrum (denoted as GMB). Thin solid lines are the reference spectrum without the vertex correction, or a mean field (MF) result. (a) $m_B/m_F = 6.67$ for a single ^{40}K atom resonating with a Fermi sea of light ^{6}Li atoms; (b)$m_B/m_F = 2.175$ or for an interspecies resonance of ^{40}K-^{87}Rb atoms; (c) $m_B/m_F = 23/6$ or ^{6}Li-^{23}Na resonance; (d)$m_B/m_F = 14.83$ or ^{6}Li-^{87}Rb resonance. In (b)–(d), minority atoms are Rb, Na, and Rb atoms respectively. Shaded areas are again for two-atom excitation continuum.

IV. IMPLICATIONS

The dispersion obtained for an individual minority atom having interspecies resonance with majority Fermi atoms that form a Fermi sea can be applied to identify the instability point[55] for an extremely imbalanced quantum Fermi-Bose or Fermi-Fermi mixture beyond which the weakly interacting mixtures become unstable. Below we assume the minority species can be either Fermi or Bose atoms with densities much lower than that of majority atoms.

The instability point corresponds to the scattering length at which the dispersion of anomalous dimers touches zero or the energy cost of creating a dimer becomes zero. Since the minimum in the dimer dispersion can be either at $\mathbf{Q} = 0$ or $\mathbf{Q} \neq 0$, it is implied that the instability might be driven by formation of dimers with either $\mathbf{Q} = 0$ or a finite $\mathbf{Q}$.

We summarize the results of the dispersion for different mixtures in Fig. 8, and the instability for different mass ratios in Fig. 9 Since the fluctuating particle-hole pairs near the Fermi surface reduce the binding energy of dimers, the formation of a dimer in the ground state for a minority atom and a Fermi sea of majority atoms occurs at a higher critical value of $1/k_F a$ when crossing the resonance from the side of negative scattering lengths. The second effect of fluctuations here appears to destabilize dimers with finite momenta near k_F, because of the peak structure in the vertex corrections. This is qualitatively consistent with the results in Fig. 9(b): The vertex corrections suppress the area of the region where Q_{min} is finite.

For the case of equal-mass interspecies resonance, the mean field calculation with a static Fermi surface yields a critical value, $(k_F a)^{-1} = 0.24$; fluctuations of particle-hole pairs correct the mean field instability point leading to a modified critical value $(k_F a)^{-1} = 0.34$. Compared to $(k_F a)^{-1} = 0.88$, the critical value obtained via the diagrammatic quantum Monte Carlo [34] that has so far been done only for the equal-mass case, our approximation yields a qualitative correct account of the main effects of fluctuations but quantitatively underestimates the effects of fluctuations. And in our diagrammatic approach, for mass ratios (m_B/m_F) less than 0.135 a dimer with finite $\mathbf{Q}$ appears in the ground state for a minority atom resonating with a Fermi sea of majority atoms at a critical value of scattering length a. This is close to 0.15, the numerical result obtained in a truncated particle-hole pair subspace [18]. However for this critical mass, the critical scattering length at which a dimer starts forming in the ground state is predicted as $(k_F a)^{-1} = 0.62$ in our approach while in Ref. [18], $(k_F a)^{-1}$ is close to a larger value of 1.7.

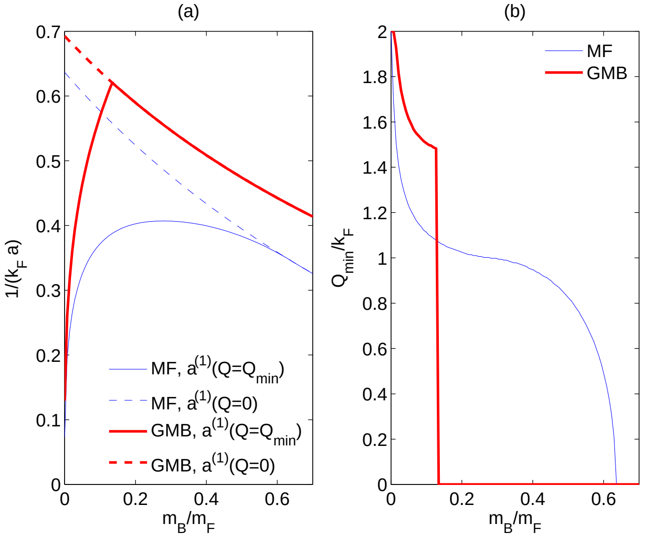

FIG. 9: (Color online) The estimated effect of particle-hole fluctuations(curve labeled as GMB) on the dimer formation; the result obtained in the static Fermi surface approximation is denoted as MF. (a) Critical line beyond which a dimer starts to appear in the ground state for a minority atom resonating with a Fermi sea of atoms; the dashed lines are obtained when only taking into account the zero-momentum dimers, i.e. set by scattering lengths at which $W_B(\mathbf{Q}=0)$ vanishes. (b) The momentum of a dimer that appears in the ground state right above the critical line.

It remains to be understood what happens beyond the instability line identified in Fig.9 and what is the nature of the transitions if there are any [56]. For Fermi-Bose mixtures, an earlier attempt was made to understand dimer correlations beyond a critical line [29] that was obtained when the scatterings in finite-$\mathbf{Q}$ channels were not included. However, the appearance of finite-density fermion dimers in the ground state beyond the critical line was not properly taken into account in analyses. This complication and more importantly potential dimer-dimer and atom-dimer interactions about which we know very little make a thorough study in this limit extremely challenging. The second issue is how dimers in a finite-$|\mathbf{Q}|$ channel compete against other structures with higher order correlations. For instance, it was also proposed that for two-dimensional Fermi-Fermi mixtures with extremely small mass ratios less than 0.01 [15], a crystal structure can further develop at exponentially low temperatures. This question perhaps can be best addressed by numerically taking into account various fluctuations. On the other hand, we remark that LOFF states have been suggested in Fermi gases near resonances. For Fermi-Fermi mixtures with equal masses, Bulgac *et al.* suggested that the ground state can be a pairing state that breaks translational symmetries [14]. Recently, it was also argued that LOFF states appear on the molecular side of resonances in almost fully polarized Fermi gases but only for nonequal masses; in addition, a trimer phase was also proposed [18]. It remains to be clarified the connections between different results obtained in Ref. [15], Ref. [14] and Ref. [18]. In Ref. [39], the authors first investigated the anomalous dispersion of molecules in Fermi-Bose mixtures and estimated the effect of fluctuating particle-hole pairs on the formation of dimers. The authors then proposed a first-order phase transition between the noninteracting ground state and a fully paired state analogous to the BCS one. Dukelsky *et al.* [57] correctly pointed out that a string factor was missing in the energetic analysis of the first-order phase transition. The correct form of the energy function should be

$$\begin{aligned} E = & \sum_{\mathbf{k}} \left(|v_{\mathbf{k}}|^2 + |\eta_{\mathbf{k}}|^2\right) \epsilon^F_{\mathbf{k}} + \sum_{\mathbf{k}} |v_{\mathbf{k}}|^2 \epsilon^B_{\mathbf{k}} \\ & + \frac{U_{bf}}{\Omega} \sum_{\mathbf{k}\mathbf{k}'} u^*_{\mathbf{k}'} v^*_{\mathbf{k}'} u_{\mathbf{k}} v_{\mathbf{k}} \times \\ & \prod_{\mathbf{k}'' \in (\mathbf{k},\mathbf{k}')} \left(|u_{\mathbf{k}''}|^2 - |v_{\mathbf{k}''}|^2 - |\eta_{\mathbf{k}''}|^2\right). \qquad (11) \end{aligned}$$

Here the string product is carried over states between $\mathbf{k}$ and $\mathbf{k}'$ in the trial wave function given in Eq.(5) in Ref. [39]. In the previous calculations, the string product was indeed overlooked and its effect was not properly taken into account. The string factor modifies the interaction energy via inducing a rapidly alternating sign when the momentum varies, and more importantly unless the distribution function is strictly the Fermi-Dirac function, the string product should be equal to zero in the thermodynamic limit where there are an infinite number of states between the two open ends of the string. For this reason, the energy of the proposed pairing states near the first-order phase transition was erroneously underestimated and within this mean field approximation with the string product properly taken into account, one is no longer able to show that there is a first-order phase transition to the proposed pairing state as argued in the previous Letter [39]. In Ref. [57], the Richardson solution has also been further utilized to argue the nonexistence of collective states below the energy of zero-momentum molecules. It was pointed out that Fermi-Bose molecules are noninteracting in the reduced pairing model employed there; in that reduced Hamiltonian that differs from the full scattering Hamiltonian [see Eq.(1)] introduced here, scatterings in all finite-Q sectors are completely suppressed. So the result of the nonexistence of lower collective modes, although it is a feature of the reduced Hamiltonian, might not be a property of cold atoms near Feshbach resonances. In fact, one can show that the second-order commutator-anticommutator for composite molecules does not vanish when the full Hamiltonian in Eq.(1) rather than the reduced pairing model is considered [58]. Two-body scattering with a finite total momentum $\hbar Q$ that was neglected in the reduced pairing Hamiltonian induces significant dimer-atom or dimer-dimer scatterings as well as scatterings between a dimer and a Fermi sea. In Fermi-Fermi mixtures, the finite-Q scattering also plays a critical role in dimer-atom or dimer-dimer scattering near resonances. The dimer or molecule dynamics near resonance can be understood when these scatterings are properly taken into account. For this reason, the issue of low-lying collective modes of the molecules remains an open question and can be addressed when the physics beyond the Richardson-solution is considered.

In summary, to understand the physics beyond the instability line, it is essential to include the two-body scattering with a finite total momentum $\hbar\mathbf{Q}$ when locating the critical scattering length for the molecule dispersion can be quite anomalous and its mass near $Q = 0$ can be negative either when far away from resonance or when the minority atom is very light. In the latter case, one can show that Fermi-Bose molecules with finite momenta should first appear in the ground state because $Q = 0$ molecules are energetically unfavorable; the instability of the noninteracting ground state is therefore driven by scatterings in finite-Q sectors rather than two-body scattering processes in the reduced pairing Hamiltonian, which excludes two-atom scattering with finite Q.

V. CONCLUSION

In conclusion, we have investigated dressed dimers in quantum mixtures and carried out thorough studies of energies of dimers in finite-$\mathbf{Q}$ channels. Our calculation suggests that in the limit of light bosons, dimers with a finite momentum $\hbar\mathbf{Q}$ are most relevant for the ground state for a minority atom resonating with a Fermi sea of majority atoms. There are two open issues that need to be understood in the future, most likely beyond the framework of the approach here. One is the role of three-body correlations in quantum mixtures. Following a general argument by Efimov, when m_B/m_F mass ratios are smaller than 0.145, trimers involving two heavy majority Fermi atoms should form in vacuum [59]. However, three-body dimer-atom resonances induced by trimers generally are much narrower than two-body resonances and contributions from Efimov physics to the two-body effective interactions can be smaller than the universal corrections that originate from collective excitations [53] which we have taken into account in this article. This was previously noticed in the studies of Fermi-Fermi mixtures [16]. In this limit, one should expect that trimers have relatively weak effects on the physics in two-body channels and that dominating effects in the dimmer channel discussed above can survive these higher order corrections.

A related and perhaps more important question is under which conditions three-body correlations are dominating and an additional trimer channel has to be added to the discussion on many-body physics. How trimers mediate additional strong scattering between dimers or dimer and atoms and lead to nontrivial higher order many-body correlations represents one of the most challenging issues we face now and remains to be studied in the future. The answer to this question should depend on short-distance behaviors of Efimov potentials and would therefore be nonuniversal. Our results about dimers should be relevant whenever these nonuniversal higher order correlations are insignificant, and the fraction of atoms forming trimers is small.

We acknowledge valuable discussions with Mikhail Baranov, Georg Bruun, Eugene Demler, Chris Greene, Rudi Grimm, Carlos Lobo, David MacNeill, Mohammad Mashayekhi, Subir Sachdev, Klaus Sengstock, Dam Thanh Son, Joseph Thywissen, Vladan Vuletic, Matteo Zaccanti, Peter Zoller, and Martin Zwierlein. One of the authors (F.Z.) would like to thank the physics department, at Harvard University and the Center for Ultracold Atoms, at MIT and Harvard for their hospitality during his visit in the winter and spring of 2011, when this article was finalized. This work is in part supported by the Canadian Institute for Advanced Research, the Izaak Walton Killam Fund for Advanced Studies, NSERC (Canada) and CUA at MIT and Harvard, and the Austrian Science Fund FWF FOCUS.

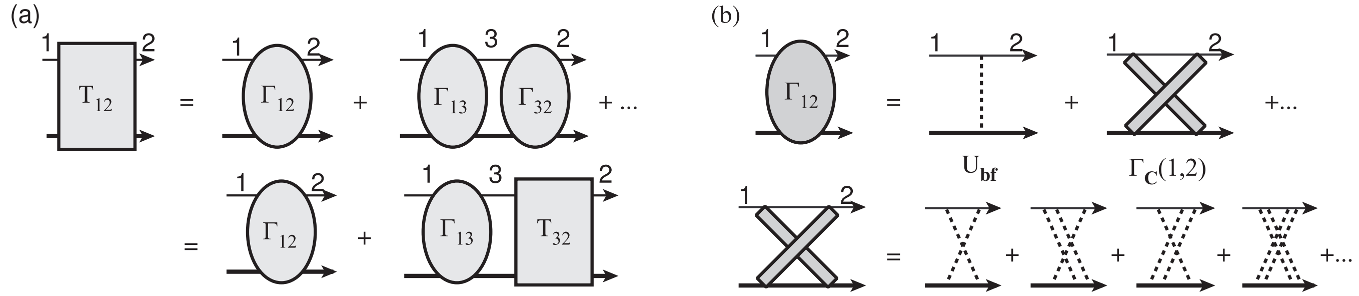

FIG. 10: Feynman diagrams for the T matrix calculation, thick (thin) solid lines are for majority (minority) atoms, dashed lines are for the bare interaction U_{bf}, and $\Gamma(\cdots)$ is the irreducible two-body interaction vertex. (a) The ladder summation and diagrammatic representation of the Bethe-Salpeter equation in Eq. (A4). (b) Γ with GMB corrections. Here the interaction lines within the $\Gamma_C(1,2)$ are renormalized interactions, which can be expanded in series of ladder diagrams using bare interaction U_{bf}.

Appendix A: T matrix in the static-Fermi-sea approximation and the molecule's effective mass

To determine the molecular excitation energy in a Fermi sea of majority atoms, we look at the T matrix for the minority-majority scattering. Diagrammatically it is the skeleton diagram (without the external propagators) of the following time-ordered two-particle propagator:

$$\langle F.S.|Tc(t,\mathbf{k}_2)b(t,\mathbf{Q}-\mathbf{k_2})b^\dagger(0,\mathbf{Q}-\mathbf{k}_1)c^\dagger(0,\mathbf{k_1})|F.S.\rangle \tag{A1}$$

where $|F.S.\rangle$ stands for the Fermi sea of majority atoms. An isolated pole of T in the energy space represents a dimer excitation. The pole could be either on the real axis or in the lower complex half plane; in the latter case the dimer has a finite lifetime. Note that the above time-ordered propagator is zero when $t<0$, because one cannot create a hole excitation of minority atoms.

In the following we use the ladder approximation to calculate T as shown in Fig.10. The rung of each ladder is the Γ function or the irreducible two-body interaction vertex, and the side rails are Green's functions of majority and minority atoms. One can write down the Bethe-Salpeter equation to include all the ladder-like diagrams as the following:

$$T(1,2) \equiv T(\omega_1,\mathbf{k}_1,E-\omega_1,Q-\mathbf{k}_1;\omega_2,\mathbf{k}_2,E-\omega_2,Q-\mathbf{k}_2) \tag{A2}$$

$$H(3) \equiv iG_F(\omega_3,\mathbf{k}_3)G_B(E-\omega_3,Q-\mathbf{k}_3) \tag{A3}$$

$$T(1,2) = \Gamma(1,2)+\sum_3 \Gamma(1,3)H(3)T(3,2) \tag{A4}$$

where we have introduced a shorthand notation $(1,2)$ to denote the incoming and outing states. Here G_F (G_B) are bare Green's functions for majority(minority) atoms defined as, $G_B^{-1}(\omega,\mathbf{k}) \equiv \omega-\epsilon^B_{\mathbf{k}}+i0^+$ and $G_F^{-1}(\omega,\mathbf{k}) \equiv \omega-(\epsilon^F_{\mathbf{k}}-\epsilon^F_F)(1-i0^+)$. In the leading order approximation, we have $\Gamma(1,2)=U_{bf}$, and one can further integrate over ω_3. The result is

$$\frac{1}{T(1,2)} = \frac{1}{U_{bf}}+\frac{1}{\Omega}\sum_{\mathbf{k}}\frac{1-n_F(\mathbf{k})}{\epsilon^F_{\mathbf{k}}+\epsilon^B_{\mathbf{Q}-\mathbf{k}}-\epsilon^F_F-E-i0^+} \tag{A5}$$

The energy of a dimer is determined from the condition that T becomes divergent when E approaches $W_B(Q)$:

$$-\frac{m_R}{2\pi\hbar^2 a} = \frac{1}{\Omega}\sum_{\mathbf{k}}\left[\frac{1-n_F(\mathbf{k})}{\epsilon^F_{\mathbf{k}}+\epsilon^B_{\mathbf{Q}-\mathbf{k}}-\epsilon^F_F-W_B(Q)}-\frac{1}{\epsilon^R_k}\right] \tag{A6}$$

The last term in Eq. (A6) was introduced to regularize the ultraviolet divergence.

The integral in Eq. (A6) can be evaluated analytically for an arbitrary value of $W_B(Q)$. And the result for the bound-state solution when $W_B(Q)<E_{th}(Q)$ is

$$1-\frac{\pi}{k_F a} = -\frac{1-2b^2+c}{4b}\log\left(\frac{1+2b+c}{1-2b+c}\right)+\sqrt{b^2-c}\left[\pi I+\mathrm{arctanh}\frac{1-b}{\sqrt{b^2-c}}+\mathrm{arctanh}\frac{1+b}{\sqrt{b^2-c}}\right] \tag{A7}$$

$$b \equiv \frac{1}{\epsilon^R_F}\frac{\hbar^2 k_F Q}{2m_B},\ c\equiv\frac{1}{\epsilon^R_F}\left(\frac{\hbar^2Q^2}{2m_B}-\epsilon^F_F-W_B\right)$$

From the above expression one can find the effective mass of the molecule m_{eff} defined as $W_B(Q)-W_B(0)\simeq\frac{\hbar^2Q^2}{2m_{eff}}$,

$$\begin{aligned}\frac{1}{m_{eff}} &= \frac{1}{m_B+m_F}-\frac{2m_R}{3m_B^2}\frac{1}{1-y^2}\frac{1}{1+\frac{1-y^2}{2y}\log\frac{1+y}{1-y}}\\ y &\equiv \sqrt{\frac{W_B(Q=0)+\epsilon_F^F}{\epsilon_F^R}} \qquad \text{(A8)}\end{aligned}$$

The effective mass at the instability point given in Eq. (6) is obtained by setting $W_B(Q=0)=0$ or $y=x=\sqrt{\frac{m_R}{m_B}}$. One can also find out that the effective mass is always negative in the limit where $\frac{1}{k_Fa}\to-\infty$ by studying the asymptotics when $y\to 1-2\exp\left(\frac{\pi}{k_Fa}\right)$:

$$\frac{1}{m_{eff}}\to-\frac{m_R}{6m_B^2}\exp\left(-\frac{\pi}{k_Fa}\right) \qquad \text{(A9)}$$

Appendix B: Effective scattering length $\tilde{a}$ From T matrix Method

In this section we use the T matrix method to study the effects of fluctuating particle-hole pairs near Fermi surface. Our analysis shows that in the limit of small k_Fa, the effects due to particle-hole fluctuations can be captured by introducing an effective scattering length $\tilde{a}$ as $\tilde{a}^{-1}=a^{-1}-k_FR+k_FO(k_Fa)$, where the function R represents the lowest order vertex correction. Similar quantities such as effective interactions have been introduced before [52], to address effects of particle-hole fluctuations in zero-momentum pairing physics. The T matrix method used here provides a unified description for dimers of different momenta and energies, and can be further extended to near resonances [51]. In the following we first show how to obtain Eq. (B7) for dimer's energy by examining the pole structure of the T matrix. Then we show how to obtain Eq. (B15) where an effective scattering length emerges.

We start from Fig.10(b), where we include the leading order term $\Gamma_C(1,2)$ as

$$\Gamma(1,2) \simeq U_{bf}+\Gamma_C(1,2) \qquad \text{(B1)}$$

$$\begin{aligned}\Gamma_C(1,2) &\simeq i\left(\frac{2\pi\hbar^2a}{m_R}\right)^2\frac{1}{\Omega}\sum_{\mathbf{l}}\int\frac{d\omega}{2\pi}G_F(\omega,\mathbf{l})G_B(\omega-\omega_1+E-\omega_2,\mathbf{Q}-\mathbf{k}_1-\mathbf{k}_2+\mathbf{l})\\ &= \left(\frac{2\pi\hbar^2a}{m_R}\right)^2\frac{1}{\Omega}\sum_{\mathbf{l}}\frac{n_F(\mathbf{l})}{E-\omega_1-\omega_2-\epsilon_F^F+\epsilon_{\mathbf{l}}^F-\epsilon^B_{\mathbf{Q+l-k_1-k_2}}+i0^+} \qquad \text{(B2)}\end{aligned}$$

Here $\Gamma_C(1,2)$ corresponds to exactly the type-A virtual process discussed in the main text. Note that in $\Gamma_C(1,2)$ we replace the renormalized interaction vertex (which is a sum of diagrams with bare interactions) for particles or holes near the Fermi-surface by two-body scattering amplitude in vacuum, i.e., $\frac{2\pi\hbar^2a}{m_R}$. This is justified in the limit of small k_Fa; such a replacement will not change function R, but only leads to inaccuracies in higher order terms. With Eq. (A4) one can write down the corresponding Bethe-Salpeter equation:

$$T(1,2) = \left[U_{bf}+\Gamma_C(1,2)\right]+\sum_3\left[U_{bf}+\Gamma_C(1,3)\right]H(3)T(3,2) \qquad \text{(B3)}$$

The above equation defines an infinite series implicitly in terms of U_{bf} and Γ_C. It is not hard to regroup terms in the series according to the powers of U_{bf} and sum them up in the following way as

$$\begin{aligned}T(1,2) &= \frac{\phi_M(1)\phi_M(2)}{U_{bf}^{-1}-\left[\sum_3H(3)+\sum_{34}H(3)\Gamma_C(3,4)H(4)+\sum_{345}H(3)\Gamma_C(3,4)H(4)\Gamma_C(4,5)H(5)+\cdots\right]}\\ &\quad+\left\{\Gamma_C(1,2)+\sum_3\Gamma_C(1,3)H(3)\Gamma_C(3,2)+\sum_{34}\Gamma_C(1,3)H(3)\Gamma_C(3,4)H(4)\Gamma_C(4,2)+\cdots\right\} \qquad \text{(B4)}\\ \phi_M(1) &\equiv 1+\sum_3\Gamma_C(1,3)H(3)+\sum_{34}\Gamma_C(1,3)H(3)\Gamma_C(3,4)+\sum_{345}\Gamma_C(1,3)H(3)\Gamma_C(3,4)H(4)\Gamma_C(4,5)+\cdots \qquad \text{(B5)}\end{aligned}$$

We can assume that the series in the curly brackets and ϕ_M are convergent, based on the estimation that each term is at most of order $(k_F a)$ compared the preceding term. Then the pole in the T matrix is completely determined by the denominator, and the dimer's energy E should satisfy the following equation:

$$\begin{aligned} \frac{1}{U_{bf}} &= \sum_{3} H(3) + \sum_{34} H(3)\Gamma_C(3,4)H(4) + \cdots && \text{(B6)} \\ &\simeq \frac{1}{\Omega}\sum_{\mathbf{k}} \frac{1-n_F(\mathbf{k})}{\epsilon^F_{\mathbf{k}} + \epsilon^B_{\mathbf{Q-k}} - \epsilon^F_F - E} + \frac{1}{\Omega^3}\sum_{\mathbf{k},\mathbf{p}} \frac{1-n_F(\mathbf{k})}{\epsilon^F_{\mathbf{k}} + \epsilon^B_{\mathbf{Q-k}} - \epsilon^F_F - E}\,\frac{1-n_F(\mathbf{p})}{\epsilon^F_{\mathbf{p}} + \epsilon^B_{\mathbf{Q-p}} - \epsilon^F_F - E} \\ &\quad \times \left(\frac{2\pi\hbar^2 a}{m_R}\right)^2 \sum_{\mathbf{l}} \frac{(-1)n_F(\mathbf{l})}{\epsilon^F_{\mathbf{k}} + \epsilon^F_{\mathbf{p}} - \epsilon^F_{\mathbf{l}} - \epsilon^F_F + \epsilon^B_{\mathbf{Q+l-k-p}} - E - i0^+} && \text{(B7)} \end{aligned}$$

Here in Eq. (B7) we have only kept leading order terms, and we have further integrated over frequencies ω_3 and ω_4.

Compared to Eq. (A5) for the static Fermi sea, the above equation is very similar except for an additional triple-momentum integral due to particle-hole fluctuations. We start to analyze this triple integral by examining the range of various denominators. We first notice that $\epsilon^F_{\mathbf{k}} + \epsilon^F_{\mathbf{p}} - \epsilon^F_{\mathbf{l}} - \epsilon^F_F + \epsilon^B_{\mathbf{Q+l-k-p}} - E$ represents the energy difference between the dimer and virtual processes, and hence can be either positive or negative depending on the values of $\mathbf{k}, \mathbf{p}, \mathbf{l}$ (one exception is at $E = 0$, the denominator is always positive for all possible k, p, l). On the contrary, the other two denominators, i.e., $\epsilon^F_{\mathbf{k}} + \epsilon^B_{\mathbf{Q-k}} - \epsilon^F_F - E$ and $\epsilon^F_{\mathbf{p}} + \epsilon^B_{\mathbf{Q-p}} - \epsilon^F_F - E$, are always positive for all possible values of $\mathbf{k}, \mathbf{p}$, which is guaranteed by the definition of bounded dimers; furthermore in the limit $k_F a \to 0^-$, these two denominators can be very close to zero as the binding energy is small. These unique features suggest that the value of the triple integral mainly depends on the value of $\sum_{|\mathbf{l}|<k_F}(\epsilon^F_{\mathbf{k}} + \epsilon^F_{\mathbf{p}} - \epsilon^F_{\mathbf{l}} - \epsilon^F_F + \epsilon^B_{\mathbf{Q+l-k-p}} - E - i0^+)^{-1}$ when $\mathbf{k}$ and $\mathbf{p}$ are near the two-body continuum threshold; i.e., $|\mathbf{k}| = |\mathbf{p}| = k_F$ (so-called "back-to-back scattering") for $Q = 0$, and $\mathbf{k} \simeq \mathbf{p} \simeq k_F\mathbf{Q}/Q$ (so-called "forward scattering") for finite $\mathbf{Q}$. Based on these considerations, one can introduce a step function approximation to simplify the dependence over $\mathbf{k}$ and $\mathbf{p}$,

$$\frac{1}{\Omega}\sum_{\mathbf{l}} \frac{n_F(\mathbf{l})}{\epsilon^F_{\mathbf{k}} + \epsilon^F_{\mathbf{p}} - \epsilon^F_{\mathbf{l}} - \epsilon^F_F + \epsilon^B_{\mathbf{Q+l-k-p}} - E - i0^+} \simeq \begin{cases} \bar{\Gamma}_C, & k_F \le |\mathbf{k}|, |\mathbf{p}| \le \Lambda_C \\ 0, & \text{otherwise} \end{cases}, \tag{B8}$$

Here $\bar{\Gamma}_C$ is a constant independent of $\mathbf{p}$ and $\mathbf{l}$. It is natural to choose $\bar{\Gamma}_C$ to be the value for "back-to-back scatterings" or "forward scatterings" as

$$\begin{aligned} \bar{\Gamma}_C(\mathbf{Q}=0, E) &= \int \frac{d\Omega_{\mathbf{n_q}}}{4\pi}\frac{d\Omega_{\mathbf{n_p}}}{4\pi}\frac{1}{\Omega}\sum_{\mathbf{l}} \frac{n_F(\mathbf{l})}{\epsilon^F_F - \epsilon^F_{\mathbf{l}} + \epsilon^B_{\mathbf{l}-k_F\mathbf{n_q}-k_F\mathbf{n_p}} - E - i0^+} && \text{(B9)} \\ \bar{\Gamma}_C(\mathbf{Q}\ne 0, E) &= \frac{1}{\Omega}\sum_{\mathbf{l}} \frac{n_F(\mathbf{l})}{\epsilon^F_F - \epsilon^F_{\mathbf{l}} + \epsilon^B_{\mathbf{Q}+\mathbf{l}-2k_F\frac{\mathbf{Q}}{|\mathbf{Q}|}} - E - i0^+} && \text{(B10)} \end{aligned}$$

where $\mathbf{n_p}$ and $\mathbf{n_q}$ are unit vectors. The effective cutoff Λ_C specifies the k or l dependence of the integral in Eq. (B8), and is estimated to be a few k_Fs in our case. In the following we will see that the specific value of Λ_C does not enter into the leading order correction. The triple-momentum integral thus can be simplified as

$$\begin{aligned} & \left(-\bar{\Gamma}_C\right)\left[\frac{2\pi\hbar^2 a}{m_R}\frac{1}{\Omega}\sum_{k_F<|\mathbf{k}|<\Lambda_C} \frac{1}{\epsilon^F_{\mathbf{k}} + \epsilon^B_{\mathbf{Q-k}} - \epsilon^F_F - E - i0^+}\right]^2 && \text{(B11)} \\ =\; & \left(-\bar{\Gamma}_C\right)\left[\frac{2\pi\hbar^2 a}{m_R}\frac{1}{\Omega}\sum_{\mathbf{k}}\left(\frac{\Theta(|\mathbf{k}|-k_F)}{\epsilon^F_{\mathbf{k}} + \epsilon^B_{\mathbf{Q-k}} - \epsilon^F_F - E - i0^+} - \frac{1}{\epsilon^R_{\mathbf{k}}}\right) + \left(\frac{1}{\epsilon^R_{\mathbf{k}}} - \frac{\Theta(|\mathbf{k}|-\Lambda_C)}{\epsilon^F_{\mathbf{k}} + \epsilon^B_{\mathbf{Q-k}} - \epsilon^F_F - E - i0^+}\right)\right]^2 && \text{(B12)} \\ \simeq\; & \left(-\bar{\Gamma}_C\right)\left[\frac{2\pi\hbar^2 a}{m_R}\left(-\frac{m_R}{2\pi\hbar^2 a} + \frac{m_R k_F}{\hbar^2}O(1)\right)\right]^2 && \text{(B13)} \\ =\; & \left(-\bar{\Gamma}_C\right)\left(1 + O(k_F a)\right) && \text{(B14)} \end{aligned}$$

Here $\Theta(x)$ is the unit step function. In Eq. (B12) we approximate E to be the mean field solution so that the first sum is $-\frac{m_R}{2\pi\hbar^2 a}$ according to Eq. (A6). The second term in Eq. (B12) is estimated of $\frac{m_R k_F}{\hbar^2}$, if $\left(\Lambda_C^2 - k_F^2\right) m_R^{-1}$ is large compared to the binding energy.

With Eq. (B12), Eq. (B13) and Eq. (B7), one arrives at the main result of this section,

$$-\frac{m_R}{2\pi\hbar^2 a} = \frac{1}{\Omega}\sum_k \left(\frac{1-n_F(k)}{\epsilon^F_k + \epsilon^B_{Q-k} - \epsilon^F_F - E - i0^+} - \frac{1}{\epsilon^R_k} \right) - \bar{\Gamma}_C(\mathbf{Q}, E) \tag{B15}$$

where the effective scattering length $\tilde{a}$ and the function R are

$$\frac{1}{k_F\tilde{a}} = \frac{1}{k_F a} - \frac{2\pi\hbar^2}{m_R k_F}\mathrm{Re}\bar{\Gamma}_C(\mathbf{Q}, E) \tag{B16}$$

$$R = \frac{2\pi\hbar^2}{m_R k_F}\mathrm{Re}\bar{\Gamma}_C(\mathbf{Q}, E) \tag{B17}$$

Several remarks about the effective lengths. First $\bar{\Gamma}_C$ is usually a complex number, with its real value leading to dimers' energy shift, and imaginary part relating to dimers' decay or finite lifetime. Here we only include the real part to obtain the energetics. Second, effective scattering lengths usually depend on energy and momentum of the pair, and we have plotted the R function for different $\mathbf{Q}$ and E in Fig.7. In the $k_F a \to 0^-$ limit when dimers are shallow, one can neglect the energy dependence and simply set $R = R(\mathbf{Q}, E = E_{th}(\mathbf{Q}))$. To extrapolate our result to near resonances, we obtain $W_B(Q)$ by solving Eq. (B15) self-consistently, and the results are shown in Fig.7(b) and Fig.8.

In the limit of large $k_F a$, the above ansatz in Eq. (B16) remains correct, although the estimate of $\bar{\Gamma}$ should include many other higher order vertex corrections which are not included in the irreducible diagrams shown in Fig.10 and is therefore more involved. Nevertheless, we expect that the diagrams in Fig.10 capture the most relevant qualitative aspect of particle-hole fluctuations. We therefore extrapolate this result to the unitary limit and apply it to atoms near interspecies resonance in Sec. III. Note also that for the dimer energetics in zero- or small-Q channels, the vertex correction appears in the lowest order and is the most dominating effect of particle-hole fluctuations. In this limit, the self-energy effect (i.e., the effective mass, the residue of the Green's function) of the minority particle appears in a higher order in terms of $k_F a$. The renormalized chemical potential does not play an important part in the discussion of the dimer; it gives an overall shift of the two-body continuum as well as the dimer's energy. We plan to study high-order effects in the future.

[1] J. R. Schrieffer, *Theory of Superconductivity* (Perseus Books, 1999).

[2] A. I. Larkin and Y. N. Ovchinnikov, Sov. Phys. JETP **20**, 762 (1965).

[3] P. Fulde and R. A. Ferrell, Phys. Rev. **135**, A550 (1964).

[4] M. G. Alford, A. Schmitt, K. Rajagopal and T. Schäfer, Rev. Mod. Phys. **80**, 1455 (2008).

[5] For an excellent review on atomic Feshbach resonances and superfluids near resonances, see C. Chin, R. Grimm, P. Julienne and E. Tiesinga, Rev. Mod. Phys. **82**, 1225 (2010).

[6] M. W. Zwierlein, A. Schirotzek, C. H. Schunck and W. Ketterle, Science **311**, 492 (2006).

[7] G. B. Partridge, W. Li, R. I. Kamar, Y.-A. Liao and R. G. Hulet, Science **311**, 503 (2006).

[8] Y.-A. Liao, A. S. C. Rittner, T. Paprotta, W. Li, G. B. Partridge, R. G. Hulet, S. K. Baur and E. J. Mueller, Nature **467**, 567 (2010).

[9] D. T. Son and M. A. Stephanov, Phys. Rev. A **74**, 013614 (2006).

[10] C.-H. Pao, S.-T. Wu and S.-K. Yip, Phys. Rev. B **73**, 132506 (2006).

[11] D. E. Sheehy and L. Radzihovsky, Phys. Rev. Lett. **96**, 060401 (2006).

[12] Z. C. Gu, G. Warner and F. Zhou, `arXiv:cond-mat/0603091`.

[13] E. Gubankova, E. G. Mishchenko and F. Wilczek, Phys. Rev. Lett. **94**, 110402 (2005).

[14] A. Bulgac and M. M. Forbes, Phys. Rev. Lett. **101**, 215301 (2008).

[15] D. S. Petrov, G. E. Astrakharchik, D. J. Papoular, C. Salomon and G. V. Shlyapnikov, Phys. Rev. Lett. **99**, 130407 (2007).

[16] M. A. Baranov, C. Lobo and G. V. Shlyapnikov, Phys. Rev. A **78**, 033620 (2008).

[17] A. Gezerlis, S. Gandolfi, K. E. Schmidt, and J. Carlson, Phys. Rev. Lett. **103**, 060403 (2009).

[18] C. Mathy, M. Parish and D. Huse, Phys. Rev. Lett. **106**, 166404 (2011).

[19] C. A. Stan, M. W. Zwierlein, C. H. Schunck, S. M. F. Raupach, and W. Ketterle,Phys. Rev. Lett. **93**, 143001(2004).

[20] A. Simoni, F. Ferlaino, G. Roati, G. Modugno and M. Inguscio, Phys. Rev. Lett. **90**, 163202 (2003).

[21] S. Inouye, J. Goldwin, M. L. Olsen, C. Ticknor, J. L. Bohn and D. S. Jin, Phys. Rev. Lett. **93**, 183201 (2004).

[22] F. Ferlaino, C. D'Errico, G. Roati, M. Zaccanti, M. Inguscio, G. Modugno and A. Simoni, Phys. Rev. A **73**, 040702 (2006).

[23] S. Ospelkaus, C. Ospelkaus, L. Humbert, K. Sengstock,

and K. Bongs, Phys. Rev. Lett. **97**, 120403 (2006).

[24] C. Ospelkaus, S. Ospelkaus, L. Humbert, P. Ernst, K. Sengstock and K. Bongs, Phys. Rev. Lett. **97**, 120402 (2006).

[25] B. Deh, C. Marzok, C. Zimmermann, and P. W. Courteille, Phys. Rev. A **77**, 010701(R) (2008).

[26] K.-K. Ni, S. Ospelkaus, M. H. G. de Miranda, A. Pe'er, B. Neyenhuis, J. J. Zirbel, S. Kotochigova, P. S. Julienne, D. S. Jin, and J. Ye, Science **322**, 231 (2008).

[27] S. Powell, S. Sachdev, H. P. Büchler, Phys. Rev. B **72**, 024534(2005).

[28] D. C. E. Bortolotti, A. V. Avdeenkov, C. Ticknor and J. L. Bohn, J. Phys. B **39**, 189 (2006).

[29] T. Watanabe, T. Suzuki and P. Schuck, Phys. Rev. A **78**, 033601 (2008).

[30] E. Fratini and P. Pieri, Phys. Rev. A **81**, 051605(R) (2010).

[31] F. Chevy, Phys. Rev. A **74**, 063628 (2006).

[32] S. Pilati and S. Giorgini, Phys. Rev. Lett. **100**, 030401 (2008).

[33] R. Combescot, A. Recati and C. Lobo and F. Chevy, Phys. Rev. Lett. **98**, 180402 (2007); R. Combescot, S. Giraud, and X. Leyronas, Europhysics Letters **88** 60007 (2009).

[34] N. Prokof'ev and B. Svistunov, Phys. Rev. B **77**, 020408 (2008).

[35] M. Punk, P. T. Dumitrescu and W. Zwerger, Phys. Rev. A **80**, 053605 (2009).

[36] C. Mora and F. Chevy, Phys. Rev. A, **80**, 033607 (2009).

[37] G. M. Bruun, A. Recati, C. J. Pethick, H. Smith and S. Stringari, Phys. Rev. Lett. **100**, 240406 (2008); G. M. Bruun and P. Massignan, Phys. Rev. Lett., **105**, 020403 (2010).

[38] Spin polarons have been studied experimentally in A. Schirotzek, C.-H. Wu, A. Sommer and M. W. Zwierlein, Phys. Rev. Lett. **102**, 230402 (2009).

[39] J. L. Song, M. S. Mashayekhi and F. Zhou, Phys. Rev. Lett. **105**, 195301 (2010).

[40] D. J. MacNeill, F. Zhou, Phys. Rev. Lett. **106**, 145301 (2011).

[41] Z. Li, S. Singh, T. V. Tscherbul, and K. W. Madison, Phys. Rev. A **78**, 022710 (2008).

[42] C. Marzok, B. Deh, C. Zimmermann, Ph. W. Courteille, E. Tiemann, Y. V. Vanne, and A. Saenz, Phys. Rev. A **79**, 012717 (2009).

[43] M. Gacesa, P. Pellegrini, R. Côté, Phys. Rev. A **78**, 010701(R) (2008).

[44] M. Taglieber, A.-C. Voigt, T. Aoki, T. W. Hänsch and K. Dieckmann, Phys. Rev. Lett. **100**, 010401 (2008); A.-C. Voigt, M. Taglieber, L. Costa, T. Aoki, W. Wieser, T. W. Hänsch, and K. Dieckmann, Phys. Rev. Lett. **102**, 020405 (2009).

[45] E. Wille, F. M. Spiegelhalder, G. Kerner, D. Naik, A. Trenkwalder, G. Hendl, F. Schreck, R. Grimm, T. G. Tiecke, J. T. M. Walraven, S. J. J. M. F. Kokkelmans, E. Tiesinga and P. S. Julienne, Phys. Rev. Lett. **100**,053201 (2008); F. M. Spiegelhalder, A. Trenkwalder, D. Naik, G. Hendl, F. Schreck and R. Grimm, Phys. Rev. Lett. **103**, 223203 (2009) A. Trenkwalder, C. Kohstall, M. Zaccanti, D. Naik, A. I. Sidorov, F. Schreck and R. Grimm, Phys. Rev. Lett. **106**, 115304 (2011).

[46] T. G. Tiecke, M. R. Goosen, A. Ludewig, S. D. Gensemer, S. Kraft, S. J. J. M. F. Kokkelmans, J. T. M. Walraven, Phys. Rev. Lett. **104**, 053202 (2010).

[47] Th. Best, S. Will, U. Schneider, L. Hackermüller, D. van Oosten, I. Bloch and D.-S. Lühmann , Phys. Rev.Lett. **102**, 030408 (2009).

[48] X. Cui, Y. Wang and F. Zhou, Phys. Rev. Lett. **104**, 153201 (2010).

[49] An illuminating discussion on the equivalence between the single-channel model and broad Feshbach resonances with a very large hyperfine coupling g can be found in C. J. Pethick and H. Smith, *Bose-Einstein condensation in dilute gases* (Cambridge University Press, 2008).

[50] L. N. Cooper, Phys. Rev.**104**, 1189 (1956).

[51] The lifetime of these anomalous molecules will be discussed in a separate paper.

[52] Practically, when a condensate is involved, one has to assume that Bose atoms have a background repulsive interaction which is strong enough that the induced interaction by Fermi atoms does not cause collapsing of the mixture. However, this should not be an issue if one is interested in Fermi-Fermi mixtures or in the limit of a single minority atom that is the focus of this paper. For more discussions on various induced interactions, see H. Heiselberg, C. J. Pethick, H. Smith and L. Viverit, Phys. Rev. Lett. **85**, 2418 (2000).

[53] L. P. Gorkov and T. M. Melik-Barkhudarov, Sov. Phys. JETP **13**, 1018 (1961).

[54] P. W. Anderson, Phys. Rev. Lett. **18**, 1049 (1967).

[55] And we will use *instability point* in the broadest sense to refer to a situation where a weakly interacting unpaired mixture becomes an excited state and will settle into a true ground state after a finite lifetime one way or the other disregarding the details of dynamics.

[56] Following the discussions about the dimer dispersion, it appears that the weakly interacting state becomes metastable near the critical line. For Fermi-Fermi mixtures, this implies a first order phase transition although a proof of it should involve a more elaborated analysis of fluctuations. Assuming the transition is of the first order, beyond the critical line toward the molecular side of the resonance, the weakly interacting Fermi mixture becomes a supercooled phase in the vicinity of the critical line or instability point but is globally unstable. This is also consistent with the first order phase transition between normal polarized electron liquids or LOFF states and BCS states in superconductors. For Fermi-Bose mixtures, the issue of the order of phase transition is more subtle depending on whether dimers form a Fermi surface and whether the atomic Fermi surface still persists up to this point thus is beyond the scope of this paper (see also the discussion at the end of the section). But if the transition is dictated by the emergence of a dimer Fermi surface, then the transition is likely of the free Fermi gas universality[27].

[57] J. Dukelsky, C. Esebbag, P. Schuck, and T. Suzuki, Phys. Rev. Lett. **106**, 129601 (2011).

[58] Using the scattering Hamiltonian in Eq. (1) rather than the reduced pairing Hamiltonian which only includes scattering in the $Q = 0$ sector, one obtains

$$\left\{\left[H,\Gamma^\dagger_\alpha\right],\Gamma^\dagger_\beta\right\} = \frac{U_{bf}}{\Omega}\sum_{\mathbf{Q}\neq\mathbf{0},\mathbf{k_1},\mathbf{k_2}} f^\dagger_{\mathbf{k_1}} b^\dagger_{\mathbf{Q}-\mathbf{k_1}} f^\dagger_{\mathbf{k_2}} b^\dagger_{-\mathbf{Q}-\mathbf{k_2}} \times$$

$$\left[\frac{1}{(\epsilon^R_{\mathbf{k_2}+\mathbf{Q}} - e_\alpha)(\epsilon^R_{\mathbf{k_2}} - e_\beta)} - \frac{1}{(\epsilon^R_{\mathbf{k_2}} - e_\alpha)(\epsilon^R_{\mathbf{k_2}+\mathbf{Q}} - e_\beta)}\right].$$

We thank Mohammad Mashayekhi for a useful discussion on this commutator.

[59] V. Efimov, Sov. Phys. JETP Lett. **16**, 34 (1972); V. Efimov, Nucl. Phys. A **210**, 157 (1973).